Sustainability in Environment
ISSN 2470-637X (Print) ISSN 2470-6388 (Online)
Vol. 3, No. 2, 2018
www.scholink.org/ojs/index.php/se

Original Paper

Multiscale Landforms Classification Based on UAV Datasets

Jean A. Doumit[1*]

[1] Department of geography, Faculty of literature and human sciences, Lebanese University, Beirut-Fanar, Lebanon

[*] Jean A. Doumit, Department of geography, Faculty of literature and human sciences, Lebanese University, Beirut-Fanar, Lebanon

Received: February 25, 2018 Accepted: March 12, 2018 Online Published: March 15, 2018

doi:10.22158/se.v3n2p128 URL: http://dx.doi.org/10.22158/se.v3n2p128

Abstract

The advance uses of Unmanned Aerial Vehicles (UAV) in geosciences by producing very high spatial resolution Digital Surface Models (DSMs), the various UAV flight altitudes led to different scales DSM. In this paper, we analyzed terrain forms using Topographic Position Index (TPI), landforms extracted by Iwahashi and Pike method and morphometric features of three different spatial resolutions DSM processed from different UAV flights height datasets of the same study area.

Topographic Position Index (TPI) is an algorithm for measuring topographic slope positions and to automate landform classifications, Iwahashi and Pike had developed an unsupervised method for classification of Landforms and we have used the techniques developed by Peuker and Douglas, a method classifying terrain surfaces into 7 classes.

Landforms extracted from the three indices listed above at the three flight heights of 120, 240 and 360 meters and compared with each other to understand the generalization of different scale and to highlight which landforms are more affected by the scale changes.

Keywords

UAV, TPI, landforms, DSM, Multi-scale

1. Introduction

The very fast evolution in technologies especially in geoinformatics, data and softwares and the appearance of Unmanned Aerial Vehicle (UAV) and their applications for digital surface extraction leads to multiscale terrain analysis. Scale is predominantly considered a function of the resolution of Digital Surface Models (DSMs) (Hengl & Evans, 2009; Mac Millan & Shary, 2009). The dependency of land surface has been confirmed by several researches (Chang & Tsai, 1991; Wood, 1996; Florinsky & Kuryakova, 2000; Evans, 2003; Hengl, 2006; Arrell et al., 2007; Deng et al., 2007; Pogorelov & Doumit,

2009; Wood, 2009).

The factor of scale plays a very important role in Landform classification different levels of measurement (nominal, ordinal, interval and ratio) this paper will discuss the terrain analysis with the applications of Terrain Position Index (TPI), Iwahashi and Pike index and the morphometric features and their effects on generalization and spatial resolutionat different UAV flights altitudes.

Pike et al. (2009) remarked that no digital elevation models derived map is definitive, as the generated parameters differs with algorithms and can vary with resolution and scale.

Landform classification stand out with terrain complexity which necessitated specific methods to quantify its shape and subdivide it into more manageable components (Evans, 1990; Gercek, 2010) which constitutes a central research topic ingeomorphometry (Pike, 2002; Rasemann et al., 2004).

An Arc Map Jenness module GIS software for landforms terrain computations was applied on three different spatial resolutions drone based DSM's for the extractions of Topographic Position Index (TPI), Iwahashi and Pike landforms and the morphometric features at different scales.

2. Study Area

On the western Lebanese mountainous chain our project location lays at an area about 2 hectares in Zaarour region (Figure 1). The chosen non urbanized mountainous area with a slight natural slope, represented by bare lands with elements of anthropogenic relief. The inclusion of anthropogenic micro-relief in the studying area due not only to the requirements of representativeness, but the presence of complicating microform for the experimental modeling of the terrain concave and convex smoothed areas.

Figure 1. Google Earth Spatio-Image of Lebanon Showing the Study Area

A Dji Phantom 3 UAV, caring a camera of 14 megapixels at a focal length of 3.61 mm used to scan the

study area at different Heights. The flight Heights are measured from the takeoff point of the UAV; the experiment constituted from 3 flight missions of 120,240 and 360 meters' height (FA-120, FA-240 and FA-360).

The three UAV missions have the same flight path designed in a mobile autopilot application called Litchi (Figure 2). The on screen display of the autopilot shows the flight path, the study area and the flight parameters (coordinates, height, time, etc.). All datasets of the three missions of different flight heights was processed in Agisoft photoscan software for the extraction of Digital Surface Models (DSM).

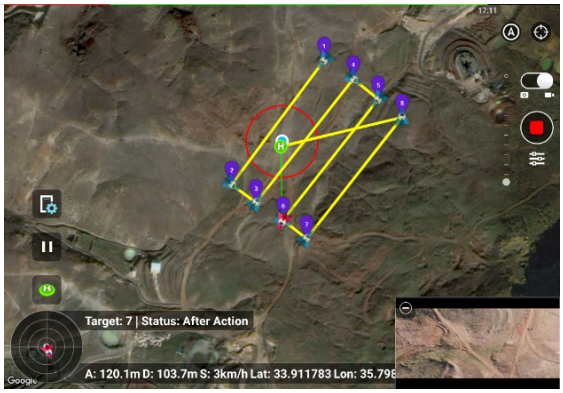

Figure 2. Designed Path of the Three Flight Missions

3. Material and Methods

Throughout the assessment, we comprehensively used this UAV for aerial images acquisition to the generation and interpretation of Digital Surface Models (DSM) by using new photogrammetry technologies.

Figure 3 shows three DSM of different spatial resolutions, FA-20 of 20 meters' flight altitude with a high resolution highlighted all the terrain details even rocks texture, passing by FA-120 the terrain is smoothed with some concave and convex areas and ending by FA-360 a very low spatial resolution and a very smoothed terrain of 360 meters' flight altitude.

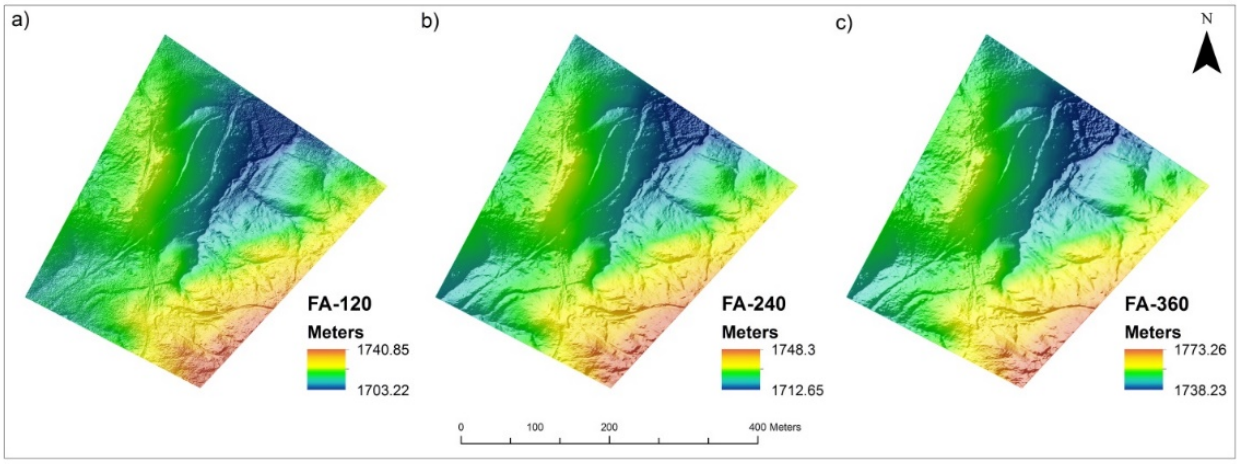

Figure 3. Multiscale DSM Extracted Based on UAV Photogrammetry, a) DSM of Flight Height 120 Meters, b) DSM of Flight Height 240 Meters, and c) DSM of Flight Height 360 Meters

These 3 DSMs can be classified visually from Figure 1, from rough to smooth, FA-120, FA-240 and FA-360 also Figure 1 constitute an interval of scales and smoothness showing the generalization at different scales.

Table 1. DSM Spatial Resolution at Different Flight Scales

DSM	Spatial resolution (m)
FA-120	1.73
FA-240	3.20
FA-360	4.47

As per Table 1 different flight altitude lead to different spatial resolutions (pixel size), as per the photogrammetry law more the flight altitude is high more the scale is small, the minimum spatial resolution is 1.73 m which express a level of details and a maximum resolution of 4.47 m with a quite good resolution for geomorphological analysis at a local scale.

Topographic Position Index (TPI), the analysis was performed by DSM's simulation to obtain Topographic Position Index (TPI). The process of formulae (1) calculate the difference between elevation at a specific cell and the average elevation of the neighborhood surrounding cells (Tagil & Jenness, 2008); describing higher and lower areas for the classification of the terrain into different morphological forms (Jenness, 2005).

The simulation required the radius adjustment of neighborhood and its geometric shape based on two different scales or two sizes (Barka et al., 2011). In this study, a radius between 5 m and 25 m was applied to determine the slope positions.

$$TPI = Z_0 - \frac{\sum_{1-n} Z_n}{n} \quad (1)$$

#

Where;

Z_0 = elevation of the model point under evaluation

Z_n = elevation of grid within the local window

n = the total number of surrounding points employed in the evaluation

These neighborhood radiuses values were applied for all DSMs spatial resolutions, to be similar in parameters for best comparison analysis.

Positive TPI values represent high locations, e.g., ridges, negative values of TPI represent low terrain representations, e.g., valleys otherwise flat areas have TPI values near zero, high positive values go to high elevations geomorphological structures such as peaks and ridges (Jenness, 2010).

The flight altitude FA-20 has a maximum positive value of 1.03, FA-60 of 0.71 and the higher flight altitude FA-360 with 0.48 a decreasing in maximum and minimum values with the increasing of flight altitude.

Iwahashi and Pike had developed a Landforms classification unsupervised method based on only three terrain attributes: slope gradient, surface texture and local convexity (Iwahashi & Pike, 2007). This method restricts a number of landform classes 8, 12 or 16 with a physical meaning of statistical landscape properties.

The unsupervised approach treats topography as a continuous random surface, especially for the three level of details FA-120, FA-240 and FA-360 independent of any spatial or morphological orderliness imposed by fluvial activity and other geomorphic processes.

Morphometric elements, the standard method for the identifcation morphological elements is to establish a mutually position for the central cell in relation to its neighbors (Peucker & Douglas, 1974; Evans, 1979). The classification algorithm can be done by maintaining the continuity of linear elements, which gives advantages over the method of selection on the basis of logical comparison of neighboring cells (Peucker & Douglas, 1974; Jenson, 1985; Bennett & Armstrong, 1989; Skidmore, 1990; Pogorelov & Doumit, 2009).

Morphological elements take the forms of: Planar, pit, channel (thalweg), pass, ridge (division line), and peak. The names of morphological elements may vary in different sources, but they can be uniquely explaining in terms of changes in the three orthogonal components x, y and z (Wood, J., 1996; Pogorelov & Doumit, 2009).

4. Results and Discussions

Landform classifications delineated using the TPI method is shown in Figure 4, TPI values present a powerful way to classify the landscape into morphological classes (Jenness, 2005). Landform Classifications consist of “Canyons, Deeply Incised Streams”, “Midslope Drainages, Shallow Valleys” and “Upland Drainages, Headwaters” all tended to have strongly negative curvature values of a

concave shape, while "Local Ridges or Hills", "Midslope Ridges, Small Hills in Plains" and "Mountain Tops, High Ridges" all tended to have strongly positive curvature values of a convex shape.

Figure 2 of the three maps shows land forms classification of all morphological forms listed above at different scale level, a visual analysis of these maps highlight a cartographic generalization between them making a very clear evolution in morphological forms at each stage.

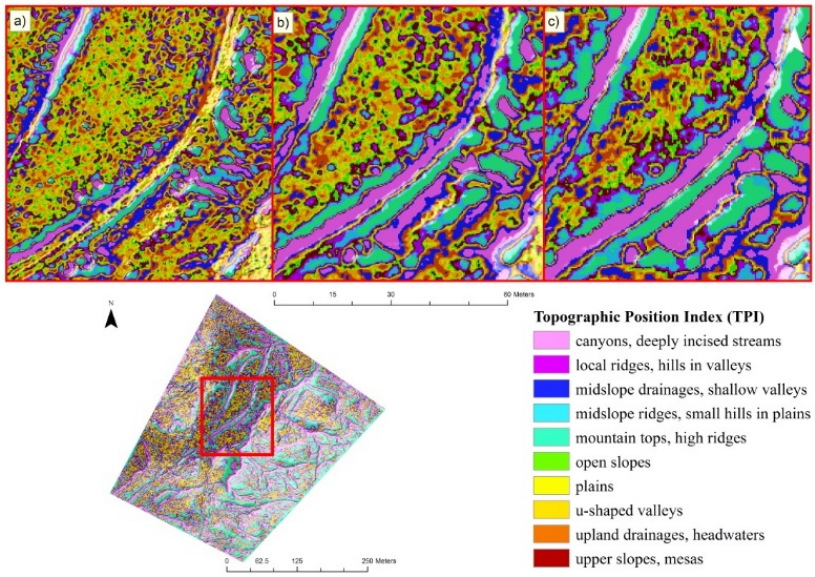

Figure 4. Maps of Landform Elements of the Three DSM Derived from TPI Classification Analysis. a) FA-120, b) FA-240, c) FA-360

The results of Table 2 shows how the area of some morphological elements is increasing against other elements relating to scale variations. In Table 3 the area percentages of some morphological elements are increasing in values and other are decreasing with the scale variation. Streams, plains, open slopes and high ridges are increasing in area and geometrical forms due to the variations in spatial resolution. Some morphological elements such as Upland drainage type are not found in any of the three maps and other like Local ridges are disappearing with scales variation and constituting a basic for generalization processes.

Table 2. Percentage of Morphological Elements and Pixels Numbers of each Morphological Element in the Three DSMs Levels Based on TPI Classification

	Area (%)			Number of pixels		
Type	FA-120	FA-240	FA-360	FA-120	FA-240	FA-360
Canyons, deeply incised streams	5.87	9.32	14.7	6155	1036	800
Midslope drainages, shallow valleys	9.75	10.6	11.46	31823	6684	5984
Upland drainages, headwaters	12.82	11.58	9.7	79684	19287	14025

U-shaped valleys	17.24	13.02	9.01	112465	29124	18901
Plains	13.1	9.69	6.39	158603	42986	22098
Open slopes	10.94	9.1	6.35	153612	42504	21892
Upper slopes, mesas	10.9	10.77	8.87	110730	30022	18910
Local ridges, hills in valleys	7.99	9.49	9.53	76494	19574	14150
Midslope ridges, small hills in plains	6.4	8.88	10.72	35575	6902	6227
Mountain tops, high ridges	4.99	7.55	13.28	6818	1663	1086
Total numbers of pixels				**771959**	**199782**	**124073**

Open slopes comprised between 6 and 11% of the total area in all flight altitudes while midslope drainages increasing with the flight heights between 9.75% and 11.46% from the total study area.

Landforms show a decreasing in their numbers; the dilution of 647886 pixels of different morphological elements from the flight height FA-120 to the flight height FA-360. All the ten morphological elements are affected by scale generalization.

To understand the degree of generalization between the big scale of FA-120 and the small scale of FA-360 we provided an ascending classification of the geomorphological forms, ridges (Local, Midslope, and high) then drainage areas (upland and midslope), hence all other morphological forms are positively affected by generalization by raising their areas.

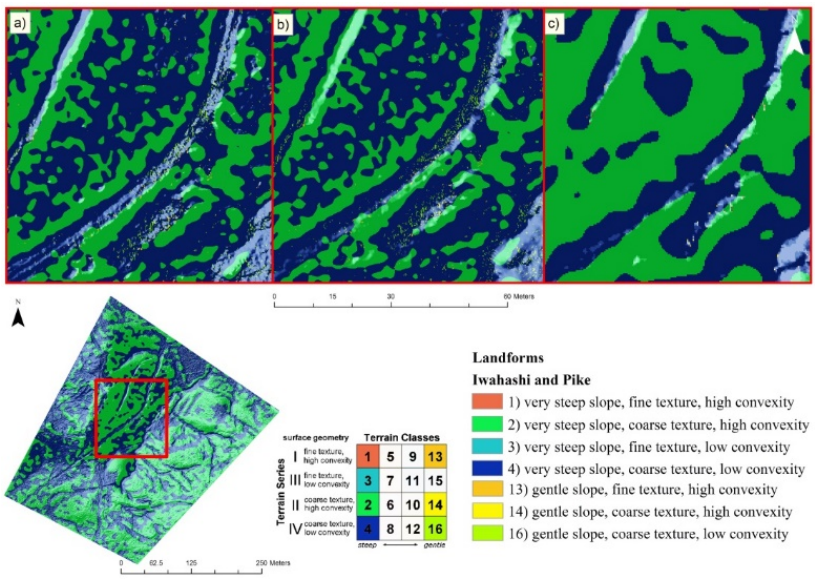

Figure 5. Landform Maps of Unsupervised Classification (Iwahashi and Pike Method), a) FA-120, b) FA-240, c) FA-360

Table 3. Iwahashi and Pike Landform Percentage of Areas at Different Scales

	Area (%)		
Type	FA-120	FA-240	FA-360
1) very steep slope, fine texture, high convexity	0.00987	—	—
2) very steep slope, coarse texture, high convexity	47.33649	48.5	49.9
3) very steep slope, fine texture, low convexity	0.00144	—	—
4) very steep slope, coarse texture, low convexity	51.13720	51.2	49.9
5) steep slope, fine texture, high convexity	—	—	—
6) steep slope, coarse texture, high convexity	—	—	—
7) steep slope, fine texture, low convexity	—	—	—
8) steep slope, coarse texture, low convexity	—	—	—
9) moderate slope, fine texture, high convexity	—	—	—
10) moderate slope, coarse texture, high convexity	—	—	—
11) moderate slope, fine texture, low convexity	—	—	—
12) moderate slope, coarse texture, low convexity	—	—	—
13) gentle slope, fine texture, high convexity	—	—	—
14) gentle slope, coarse texture, high convexity	0.67723	0.2	0.1
15) gentle slope, fine texture, low convexity	—	—	—
16) gentle slope, coarse texture, low convexity	0.83771	0.2	0.1

The concavity and convexity of the very steep slope with fine texture found only in high spatial resolution models (FA-120), the coarse texture of high convexity increasing with the pixel size.

Step and moderate slopes are not detected in all three models, gentle slope coarse texture high and low convexity are increasing with the flight altitude.

Varying DSM spatial resolution can achieve an elements separation of appropriate scale, without the need of generalization.

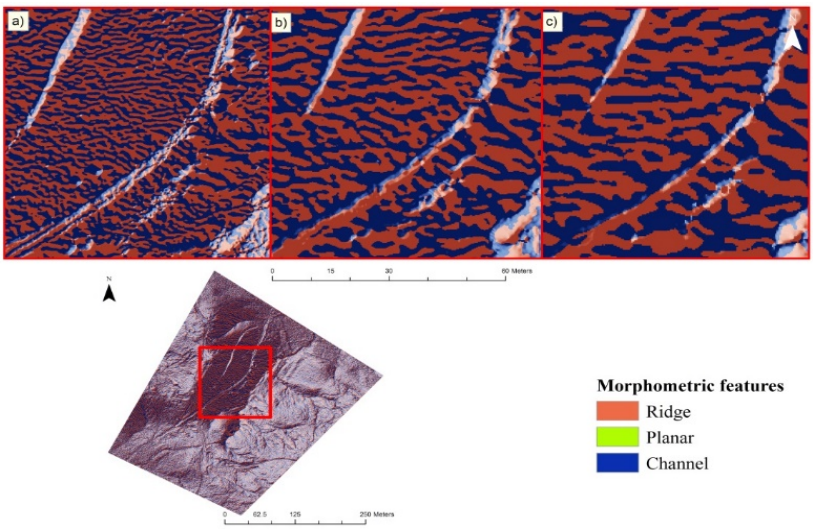

Figure 6. Morphometric Features Maps, a) FA-120, b) FA-240, c) FA-360

Table 4. Surface Specific Points Area Percentages of the Study Area at Different Scales

	Area (%)		
Type	FA-120	FA-240	FA-360
Planar	0.00001	—	—
Pit	—	—	—
Channel	49.72501	48.3	47.4
Pass (saddle)	—	—	—
Ridge	50.27497	51.7	52.6
Peak	—	—	—

As per Table 4 some morph metric features like pit, pass and peak are not detected in all flight altitudes, otherwise planar areas are detected in FA-120 the lower flight altitude at a very low percentage of area in order of 0.00001%, we cannot judge on this result because the value of this pixel could be a processing artifact. The area of channels is increasing with the flight altitude and the ridge area is decreasing against the channel one.

The dominating land forms of surface specific points channel and ridges of the study area form a comparison models of each flight height with TPI land forms. By splitting channels and Ridges of FA-120, FA-240 and FA-360 and exanimating which TPI land forms are included in each type, Table 5 shows the area percentage of each landform.

Table 5. Percentage of TPI Landforms Containing in Ridges and Channels at Each Flight Altitude

TPI Landforms	Percentage of area					
	Ridge-120	Channel-120	Ridge-240	Channel-240	Ridge-360	Channel-360
Canyons, deeply incised streams	1.5	10.4	2.4	16.8	4.3	26.3
Midslope drainages, shallow valleys	3.3	16.3	3.9	17.8	4.9	18.6
Upland drainages, headwaters	5.7	19.7	5.4	18.0	5.6	14.4
U-shaped valleys	11.9	23.1	9.3	17.1	7.0	11.2
Plains	13.7	12.4	9.6	9.6	6.3	6.5
Open slopes	14.7	7.1	11.4	6.8	7.1	5.4
Upper slopes, mesas	16.5	5.3	15.3	5.7	11.5	6.0
Local ridges, hills in valleys	12.9	3.0	14.9	3.7	13.8	4.9
Midslope ridges, small hills in plains	10.7	1.9	14.6	2.7	16.8	3.9
Mountain tops, high ridges	9.1	0.9	13.1	1.6	22.7	2.9

Upper slopes areas in ridge-120 and ridge-240 occupied a high percentage of areas, for ridge-360 the higher percentage of area goes to Mountain tops. Upland drainage owns high values in channel FA-120 and FA-240 but for FA-360 the higher area goes to Canyons. From these results we can see a TPI landform transition with scales.

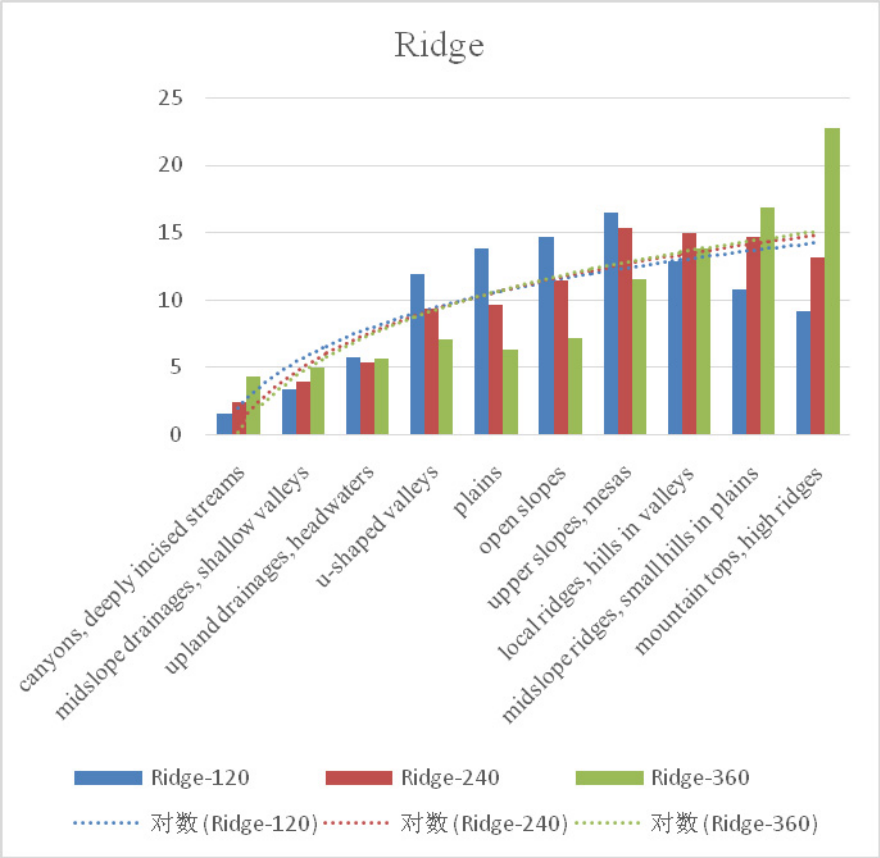

Figure 7. Diagram of Area Percentage of TPI Landforms Containing in Ridge at Flight Altitudes of 120,240 and 360 Meter

The diagram of Figure 7 shows the percentage of TPI land forms area in ridges at different scales, the log curves of 120, 240 and 360 have an intersection point at upper slope this point made a transition of values from low percentage to higher percentage of areas.

The correlation value of R^2 between land forms of FA-120 is 0.6 for FA-240 is 0.9 well correlated because of the proportionality and small percentage interval of areas, for FA-360 the correlation value is 0.6 similar to FA-120.

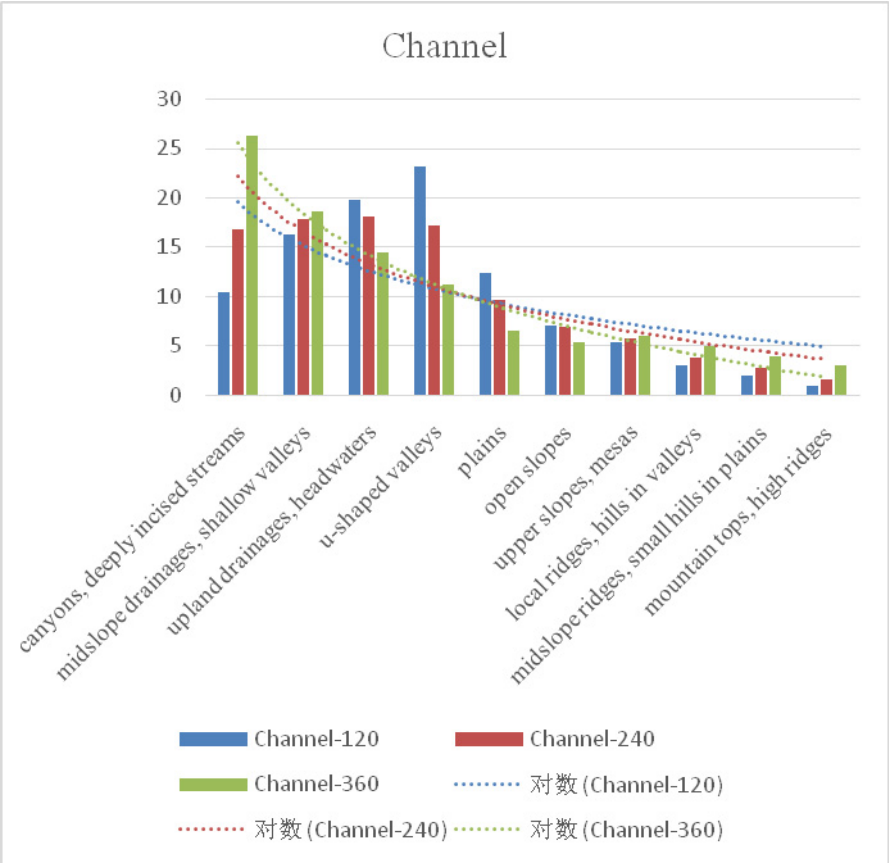

Figure 8. Diagram of Area Percentage of TPI Landforms Containing in Channel at Flight Altitudes of 120, 240 and 360 Meter

Channel usually are concave areas, in Figure 8 we can see dominating the area of canyons in FA-360, the correlation of area percentage between the landforms of FA-360 is very high with $R^2 = 0.97$ and a concave logarithmic trend line.

Otherwise for FA-240 a less concavity logarithmic trend line with $R^2 = 0.75$ due to the proportional percentage of areas between landforms.

Fa-120 has a low correlation between landforms $R^2 = 0.35$ even less than the average. We can conclude from these values that due to cartographic generalization and the transition from flight altitude to other, the degree of similarity for channels landforms areas rising with the flight altitude. Hence for ridges land types the area of canyons and midslope, upper slope local ridge, midslope ridge and mountain tops are increasing with flight altitude, upland drainage, u-shaped valley, plain and open slope area is decreasing with the flight heights.

5. Conclusion

In this study, drone Digital Surface Models (DSM) at diverse flight heights used as input data. By using Topographic Position Index and unsupervised classification of Iwahashi and Pike, the study area was classified into landform categories of different scale DSM. The result shows that ridges and drainage

forms are more affected to generalization than other forms.

The landform classes obtained for the three scales differentiate dynamic terrain characteristics of the study area. Landform classifications extracted form drone DSM and GIS fast the presented results and discussion by integrating the geospatial multiscale approach of terrain analysis.

The result shows that TPI provided a powerful tool for describing topographic attributes of a study area and there is a relationship between landform map and spatial resolution. By deep understanding of the terrain characteristics, potential and specific constraints of cartographic generalization. Information and methods discussed in this paper are valuable results for cartographicmultiscale studies and analysis. Landforms are dissolving with scales against each other's, some of them gaining areas and some disappeared. This paper analyzed the generalization at three different scales (flight altitude), for future researches we are planning to examine and monitor changes of landforms at micro, local and global scales.

References

Arrell, K., Fisher, P. F., Tate, N. J., & Bastin, L. (2007). A fuzzy c-means classification of elevation derivatives to extract the morphometric classification of landforms in Snowdonia, Wales. *Computers & Geosciences*, *33*, 1366-1381. https://doi.org/10.1016/j.cageo.2007.05.005

Barka, I., Vladovic, J., & Malis, F. (2011). *Landform classification and its application in predictive mapping of soil and forest units*. Proceedings: GIS Ostrava 2011.

Chang, K., & Tsai, B. (1991). The effect of DEM resolution on slope and aspect mapping. *Cartography and Geographic Information Science*, *18*, 69-77. https://doi.org/10.1559/152304091783805626

Deng, Y., Wilson, J. P., & Bauer, B. O. (2007). DEM resolution dependencies of terrain attributes across a landscape. *International Journal of Geographical Information Science*, *21*, 187-213. https://doi.org/10.1080/13658810600894364

Evans, I. (2003). Scale-specific landforms and aspects of the land surface. In I. S. Evans, R. Dikau, E. Tokunaga, H. Ohmori, & M. Hirano (Eds.), *Concepts and Modelling in Geomorphology: International Perspectives* (pp. 61-84). Terrapub, Tokyo.

Evans, S. (1990). General Geomorphometry. In A. S. Goudie, M. Anderson, T. Burt, J. Lewin, Richards, K. Whalley, & B. Worsley (Eds.), *Geomorphological Techniques* (2nd ed., pp. 44-56). Unwin Hyman, London.

Florinsky, I. V., & Kuryakova, G. A. (2000). Determination of grid size for digital terrain modelling in landscape investigations-exemplified by soil moisture distribution at a micro-scale. *International Journal of Geographical Information Science*, *14*, 815-832). https://doi.org/10.1080/136588100750022804

Gerçek, D. (2010). *Object-based classification of landforms based on their local geometry and geomorphometric*.

Hengl, T. (2006). Finding the right pixel size. *Computers & Geosciences*, *32*, 1283-1298.

https://doi.org/10.1016/j.cageo.2005.11.008

Hengl, T., & Evans, I. S. (2009). Mathematical and digital models of the land surface. In T. Hengl, & H. I. Reuter (Eds.), *Geomorphometry—Concepts, Software, Applications. Developments in Soil Science* (Vol. 33, pp. 31-63). Elsevier, Amsterdam. https://doi.org/10.1016/S0166-2481(08)00002-0

Iwahashi, J., & Pike, R. J. (2007). Automated classifications of topography from DEMs by an unsupervised nested-means algorithm and a three-zone geometric signature. In *Geomorphology* (Vol. 86, No. 3/4, pp. 409-440). https://doi.org/10.1016/j.geomorph.2006.09.012

Jenness, J. (2005). *Topographic Position Index*. Extension for ArcView 3.x. Retrieved from http://jennessent.com

Jenness, J. (2010). *Topographic Position Index (tpi_jen.avx) extension for ArcView 3.x* (Vol. 1.3a). Jenness Enterprises. http://www.jennessent.com/arcview/tpi.htm.

MacMillan. R. A., & Shary, P. A. (2009). Landforms and landform elements in geomorphometry. In T. Hengl, & H. I. Reuter (Eds.), *Geomorphometry—Concepts, Software, Applications. Developments in Soil Science* (Vol. 33, pp. 227-254). Elsevier, Amsterdam. https://doi.org/10.1016/S0166-2481(08)00009-3

Pike, R. J. (2002). A bibliography of terrain modeling (geomorphometry), the quantitative representation of topography-supplement 4.0., Open-File Rep. No. 02-465. *U.S. Geological Survey, Denver* (p. 116).

Pogorelov, A. V., & Doumit, J. A. (2009). *Relief of Kuban river basin: Morphometric analysis* (p. 208). M.: Geoc. (In Russian).

Rasemann, S., Schmidt, J., Schrott, L., & Dikau, R. (2004). Geomorphometry in mountain terrain. In M. P. Bishop, & J. F. Shroder (Eds.), *GIS & Mountain Geomorphology* (pp. 101-145). Springer, Berlin.

Tagil, S., & Jenness, J. (2008). GIS-based automated landform classification and topographic, Landcover, and geologic attributes of landforms around the Yazoren Polje, Turkey. *Journal of Applied Sciences*, *8*(6). 910-921. https://doi.org/10.3923/jas.2008.910.921

Wood, J. (1996). *The geomorphological characterization of digital elevation models* (PhD Thesis). University of Leicester.

Wood, J. (2009). Geomorphometry in LandSerf. In T. Hengl, & H. I. Reuter (Eds.), *Geomorphometry—Concepts, Software, Applications* (Vol. 33, pp. 333-349). Elsevier, Amsterdam. https://doi.org/10.1016/S0166-2481(08)00014-7